Impact of plasma response models in three-dimensional fluid modeling of divertor heat fluxes in RMP ELM control scenarios at ITER

O. Schmitz[1,2], M.Becoulet[3], P. Cahyna[4], T. Evans[5], Y. Feng[6], N.M.Ferraro[5], H.Frerichs[1,2], G.Huijsmans[7], L.Lao[5], A.Loarte[7], D.Reiter[2]

[1]*University of Wisconsin – Madison, Department of Engineering Physics, Madison, WI, 53706, USA*
[2]*Institut für Energieforschung - Plasmaphysik, Forschungszentrum Juelich GmbH in der Helmholtz-Gemeinschaft, Jülich, Germany*
[3]*CEA/IRFM, Cadarache, 13108 St. Paul-lez-Durance Cedex, France*
[4]*IPP AS CR, Za Slovanou 3, 18200 Prague 8, Czech Republik*
[5]*General Atomics, San Diego, California, USA*
[6]*Max-Planck Institute for Plasma Physics, Greifswald, Germany*
[7]*ITER Organization, Toute de Vinon sur Verdon, 13115 St. Paul-lez-Durance Cedex, France*

1. Introduction

Application of resonant magnetic perturbation (RMP) fields is considered at ITER for the control of Edge-Localized Modes (ELMs) [1]. During RMP ELM suppression at DIII-D heat and particle fluxes are rearranged into a three-dimensional (3D) pattern [2]. Recently a direct link between the formation of this 3D plasma boundary and the internal plasma response to the external RMP field has been shown [3]. This highlights the importance for understanding the coupling between plasma response and plasma transport in the very edge and down to the divertor target surfaces. In this contribution, the consequences of three different plasma response models on the 3D boundary formation and on the divertor heat flux at ITER are briefly discussed. The 3D fluid plasma and kinetic neutral transport code EMC3-Eirene [4] is used for edge transport modeling. The plasma response modeling is conducted with the M3D-C1 code [5] using first a single fluid, non-linear MHD model and second a two fluid, linear MHD model. This approach is referenced to an ideal MHD like screening model [6] based on resonant field damping factors obtained from the cylindrical, non-linear two-fluid MHD model RMHD [7].

2. Magnetic topology with single fluid, non-linear MHD

In this section, the magnetic topology for the M3D-C1 plasma response solutions considered is presented. We focus on the non-linear, single fluid M3D-C1. The magnetic equilibrium of a standard ITER H-mode discharge at plasma current of 15MA, magnetic field of 5.3T and a pedestal electron temperature constrain of 4.4keV is used. The magnetic perturbation field applied is a toroidal mode number n=3 harmonic field at 45kAt current in the ELM control coils and a toroidal phase alignment optimized for maximum island overlap [8]. A linear, two-fluid solution from M3D-C1 is considered in the EMC3-Eirene modeling discussed in section 3. Here we present in figure 1, the connection length map around the perturbed X-point structure (upper plots) with vacuum fields on the left and magnetic fields from M3D-C1 linear, two fluid MHD on the right.

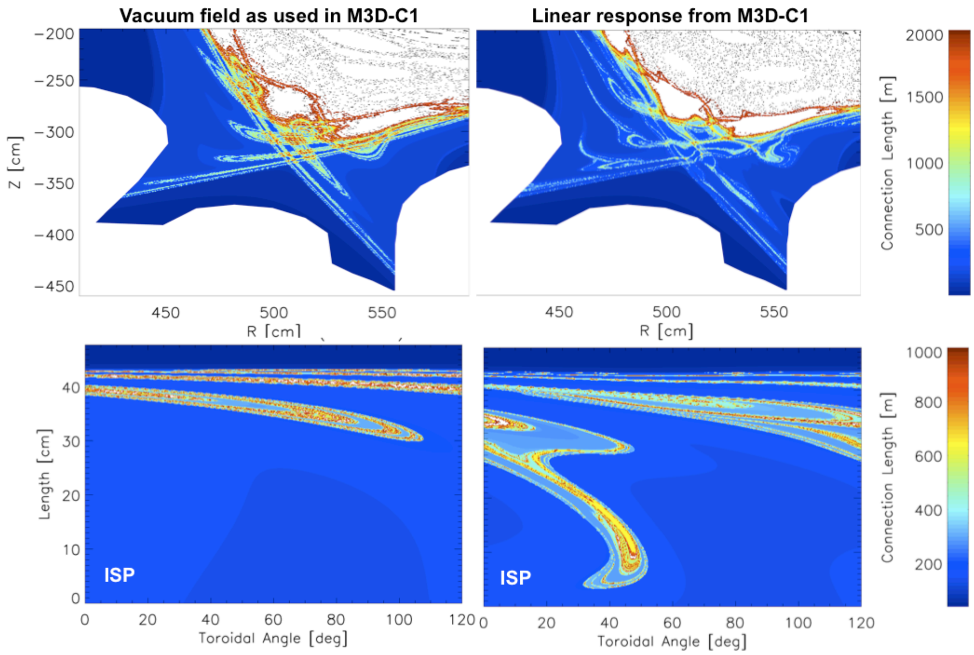

Figure 1: Magnetic topology for the linear, two fluid M3D-C1 solution - magnetic connection length at the X-point (upper plots) and magnetic footprint at the inner strike point (lower plots).

Formation of an island chain with fragmented flux surfaces of field lines with long connection length is seen for both magnetic fields. Helical fingers are formed in the vacuum field case, which reach out to the wall but touch the wall only very close to the unperturbed strike line location at this toroidal position. The additional magnetic field in the linear response case originates from current sheets of screening response and they yield an additional perturbation of the separatrix structure. The invariant manifolds get broadened and shows a more complex and anisotropic structure. The original lobe structure is maintained but now surrounded by a mesh of thin and highly perturbed fingers. In particular the second lobe at the inner strike point now touches the material surface in a broadened lobe structure. This feature is also seen in the magnetic footprint on the target surface (lower plots). For the linear response case, in general a broadening of the helical lobes and in particular a strong additional excursion of the outermost lobe is seen. The effect of the plasma response on the outer divertor structure is small. In general the implementation of plasma response from M3D-C1 does not reduce the level of stochasticity and has a small impact only on the width and helical extension of the striated footprint pattern. This result is in strong contrast to the results obtained earlier [9] using a plasma response model based on cylindrical extended MHD modeling [6]. With this model, including the plasma response resulted in a strongly reduced island size and a strong compression of the helical lobes towards the unperturbed separatrix structure.

3. Impact of plasma response on divertor heat flux

The heat divertor fluxes are analyzed including both plasma response models applied.

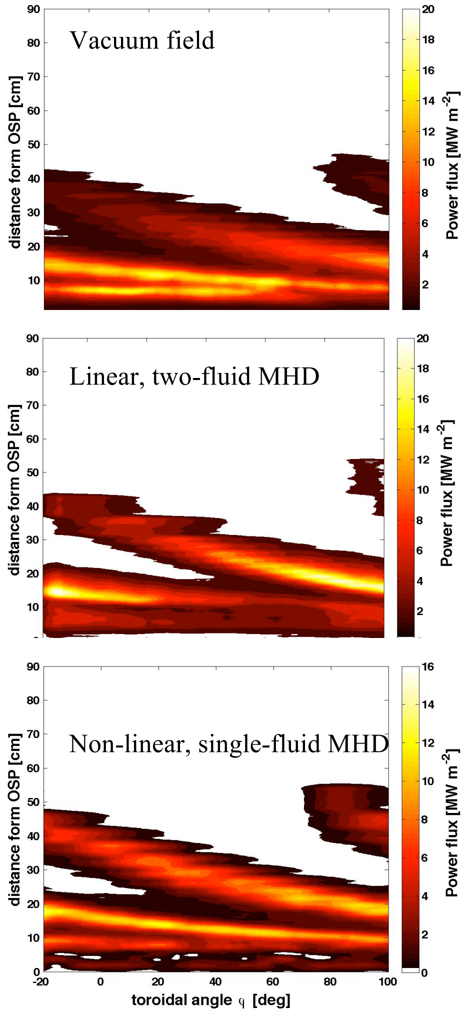

Figure 2: Heat flux pattern at **outer strike point** domain for vacuum fields (top plot) and magnetic fields obtained from **M3D-C1 linear, two fluid solution** (middle) from **M3D-C1 non-linear, single fluid solution** (bottom figure).

The boundary conditions used for EMC3-Eirene are for perpendicular transport coefficients $D_\perp$=0.4m^2/s and $\chi_\perp$=1.2m^2/s, heating power P_H=100 MW, recycling flux at target plates Γ_{rec}=150 kA and core particle source Qc=3.6kA. A medium density, low temperature divertor regime ($n_e \sim 10^{20}$ m^{-3} and $T_e \sim$ 15 eV) is obtained and no impurity radiation was included.

The heat flux into the helical lobe structure at the outer divertor leg is shown in figure 2. From top to bottom, we display the modeling result for the vacuum magnetic field case, the linear, two-fluid response and the non-linear, single fluid plasma response. The impact of the plasma response on the eventual heat flux structure and magnitude is small. Even in spite of the considerable modification of the perturbed X-point structure and magnetic footprint discussed in the previous section, the alteration of the heat flux structure is negligible. The only apparent change is the fact that the heat flux maxima is for both response cases shifted radially outward towards the tip of each lobe. The internal plasma response currents seem to shift the field line dynamics such that a stronger outward directed energy flow into the helical lobes occur. This results in a displacement of the heat flux maxima away from the unperturbed strike line location. This is again in strong contrast to the results obtained earlier [9] with an ideal MHD like screening model where the heat flux striation was strongly reduced and a increased of peak heat fluxes close to the unperturbed strike line location was obtained.

4. Conclusions

The linear, two-fluid and non-linear, single fluid MHD solutions obtained with M3D-C1 and used in the EMC3-Eirene modeling generates a perturbed magnetic field structure, which is globally very comparable to the correspondent vacuum case. Heat and particle fluxes are similar as far as the peak values are concerned but a spreading of the divertor fluxes into the 3D helical SOL is consistently seen when the plasma response is included. This result is in strong contrast to earlier analysis outcome with an ideal MHD like screening response. Here, a strong screening was used based on non-linear cylindrical MHD modeling. This screening resulted in cancelation of almost all resonant plasma components. Here, a strong reduction of the heat flux width was seen with an enhanced local peaking of heat and particle fluxes at the unperturbed strike line location.

Identification of key aspects and validation of plasma response and 3D edge transport modeling against experimental data is an urgent task to identify which plasma response trends in agreement with experiment. Understanding the plasma response with direct (magnetic) measurements rather then through the interface of complicated 3D edge transport and plasma wall interaction is a key task in this regard.

Acknowledgement: This work was supported in part by the ITER organization (under Task Agreement C19TD41FE and Contract IO/CT/11/4300000497).

References

[1] A. Loarte et al., *Nuclear Fusion,* **54** (2014) 03307
[2] T.E. Evans et al., *L. Phys.: Conf. Series,* **7** (2005) S109-121
[3] O. Schmitz et al., *Nuclear Fusion,* **54** (2014) 012001
[4] Y. Feng et al., *Contrib. Plasma Phys.,* **44** (2005) 25
[5] N. Ferraro et al., *Physics of Plasmas*, **19** (2012) 056105
[6] P. Cahyna et al., *Journal of Nuclear Materials*, **415** (2011) S927-S931
[7] M. Becoulet et al., *Nuclear Fusion*, **52** (2011) 054003
[8] T.E. Evans et al., *Nuclear Fusion,* **53** (2013) 093029
[9] O. Schmitz et al., *Journal of Nuclear Materials*, **438** (2013) S194-S198